DEM Resolutions for Landslide Susceptibility Modeling

Azemeraw Wubalem (✉ alubelw@gmail.com)

University of Gondar, Ethiopia

Abstract

In landslide susceptibility mapping, the digital elevation model (DEM) is one of the most essential data sets, which is frequently used. Therefore, evaluate the effects of the spatial resolution of DEM on the landslide susceptibility model is very important. Hence, this paper is analyzed only the effects of the spatial resolution of DEM, Advanced Spaceborne Thermal Emission, and Reflection (ASTER) was used for DEM data source. The ASTER DEM was resampled to 45, 60, 75, and 90 m spatial resolutions. A set of geodatabases were built using Geographic Information System (GIS), which contains landslide governing factors and landslide inventory. Frequency ratio (FR) and certainty factor (CF) statistical methods were employed to generate a landslide susceptibility map. Landslide density and area under the curve (AUC) were applied to evaluate the model's performance for each DEM resolution. The results of the predictive rate curve value of AUC showed a coarser DEM resolution (90 m) produced the best performance and prediction accuracy. This indicated that a coarser DEM resolution produced higher predictive accuracy than fine resolution. Concerning the statistical models, the frequency ratio model produced very good accuracy at the coarser DEM resolutions (75 and 90 m). The predictive rate curve value of AUC ranges from 86-92% for the FR model and 81-89% for the CF model which indicating very good accuracy of the models to predict future landslide incidence in the study area. Therefore, it is possible to endorse statistical methods (frequency ratio, and certainty factor) respect with to DEM resolution, which is satisfactory to landslide susceptibility mapping.

Introduction

Landslides can be defined as the mass moments of soil, rock, debris, or earth down a slope under the influence of the force of gravity (Brunsden 1979; Cruden 1991). Although rainfall, anthropogenic activity, and earthquake are the main triggering factors for landslide occurrence, complex geological conditions, geomorphological conditions, surface process, and hydrological conditions are factors that strongly influenced landslide occurrence in Ethiopia (Kifle 2013; Wubalem and Meten 2020). Landslide is becoming the most destructive geo-hazards in the hilly and mountainous parts of north, south, northwestern and central Ethiopia that resulted in the loss of life, economic loss, destruction of cultivated and non-cultivated land, destruction of engineering structures, and environmental disruption. In the last two years, from 2018 - 2020, rainfall triggered landslides also caused 120 people to die, 60 people to injure, 8,091 households to displace, houses to damage, and to destruct widely cultivated and non-cultivated lands in different parts of the country. The study area is one of the areas that frequently affected by rainfall-triggered landslide incidences. Landslide in this area resulted in the damage of houses, farmlands, and the loss of animal and human lives. Preparing of landslide susceptibility map in this region is very essential to reduce the damages by landslide incidence. However, prediction modeling of landslide susceptibility depends on a multifaceted environment of many scales dependent on landslide-governing factors including geomorphologic features, geological features, hydrological/climatic features, geodynamic and anthropogenic conditions in a given terrain. For example, geomorphological features slope, aspect, curvature, and hydrologic feature distance to drainage and drainage density can

drive from Digital Elevation Model (DEM). The prediction accuracy of the landslide susceptibility model highly depends on the resolution of DEM. Therefore, proper DEM resolution selection is one of the most important elements in landslide susceptibility modeling followed by landslide inventory mapping. However, it depends on the average size of a landslide in a given Terrain.

In literature, landslide susceptibility mapping conducted considering fine and coarse DEM resolution (Dietrich and Montgomery 1998; Li and Zhou 2003; Lee et al. 2004). Hence landslides occur as large to very large sizes, fine DEM resolution could not necessarily result in high prediction accuracy in landslide susceptibility mapping (Mahalingan and Olsen 2016; Mahalingan et al. 2016; Pradhan and Sammen 2017). Because the fine DEM resolution enhanced detailed morphometric features than a large landslide, morphometric features. Li and Zhou (2003) were conducted a landslide susceptibility modeling considering fine and coarse DEM resolution (5, 10, 20, 40, and 80 m) and conclude fine DEM resolution (20m) received the highest accuracy. Similarly, landslide susceptibility modeling conducted considering 2 to 40m and 5 to 25 m DEM resolution by Palamakumbure et al. (2015) and Schogel et al (2018), respectively. They concluded that the highest predictive accuracy was received at 10m DEM resolution. Nevertheless, Tarolli and Tarboton (2006) conducted landslide susceptibility modeling considering 2 to 50m DEM resolution and found the fine resolution of DEM less than 10m does not represent the physical process responsible for landslide occurrence due to extreme detail in terrain features. In the same way, Catani et al (2013) did landslide susceptibility modeling using fine and coarse DEM resolution and found fine DEM resolution received lower prediction accuracy than coarse DEM resolution. Tian et al (2008) conducted a landslide study considering 5 to 90m DEM resolution and found coarse DEM resolution (90m) received the highest prediction accuracy. Similarly, Zhou et al. (2020) conducted landslide susceptibility mapping considering fine and coarse DEM resolution (30, 40, 50, 60, 70, 80, and 90) and found coarse DEM resolution (70m) received the highest prediction accuracy. Whatever the results of the prediction accuracy of the landslide susceptibility model considering fine and coarse DEM resolution, the effects of DEM resolution depend on the average sizes of a landslide in a region (Lee et al 2010). The fine DEM resolution is more appropriate for small average landslide size whereas coarse DEM resolution is appropriate for relatively large average landslide size.

There are several approaches established for landslide susceptibility mapping and they are broadly classified as quantitative and qualitative models. The use of mapping techniques for landslide susceptibility mapping highly depends on the local environmental condition, triggering factors, types of the landslide, and availability of data (Yilmaz 2009). Qualitative methods required well-experienced experts and the analysis was performed based on the expert opinions and the intrinsic properties of landslides (Ayalew and Yamagishi 2005). The analytical hierarchy process (AHP) and weight linear combination are examples of qualitative methods. Quantitative methods are classified into deterministic, data mining, and statistical methods. The deterministic methods are numerical modeling which can apply when the intrinsic properties of the ground condition are homogeneous and the study area is relatively small. The statistical methods widely used throughout the world and provide reliable results (Varnes 1984; Dai and Lee 2002; Donati and Turrini 2002; Ayalew and Yamagishi 2005; Duman et al. 2006; Regime et al. 2014; Meten et al. 2015; Chandak et al. 2016; Zhang et al. 2017; Kouhpeima et al.

2017; Wubalem and Meten 2020). The statistical methods such as bivariate and multivariate methods are very important to develop a statistical relationship between landslide events and landslide governing factors as well as to predict future landslide occurrence (Guzzetti et al. 1999; Yilmaz 2009; Sakar et al. 2013; Chandak et al. 2016; Zhang et al. 2017; Kouhpeima et al. 2017; Wubalem and Meten 2020). Bivariate statistical methods are applicable based on the statistical relationship between landslide governing factors and density of landslide in a region (Chen and Wang 2007; Jia et al. 2010; Karimi et al. 2010; Pradhan et al. 2011; Ciampaline et al. 2016). Frequency ratio, information value, certainty factor, the weight of evidence are examples of bivariate statistical methods. They can help to evaluate the statistical contribution of each factor classes using the GIS tool (Chung and Fabbri 2003, 2005; Saha et al. 2005; Sarkar et al. 2006; Lee and Pradhan 2006, 2007; Akgun et al. 2008; Kanungo et al. 2009; Pradhan et al. 2010c, 2011, 2012; Kanungo et al. 2011; Pourghasemi et al. 2012a; Sujatha et al. 2012; Pourghasemi et al. 2013c; Liu et al. 2014; Qiqin et al. et al. 2019; Zine et al. 2019). A multivariate statistical method helps to determine the statistically significant landslide factors which include logistic regression and discrete analysis (Ayalew and Yamagishi 2005; Yalcin et al. 2011; Meten et al. 2015; Wubalem and Meten 2020; Zhou et al. 2020). In recent times, advanced data mining methods have been widely used in landslide susceptibility modeling, including random forest, boosted regression tree, classification and regression tree, Naïve Bayes, support vector machines, kernel LR, logistic model tree, index of entropy, and artificial neural networks. However, data mining methods are time-consuming, are incapable to determine the effects of each landslide factor class, and require high computing capacity, and the internal calculation process of these methods is intensive and cannot easily be understood (Wubalem 2020). Although there is a bit little difference in the degree of predictive accuracy, both statistical and data mining methods provide reliable predictive accuracy

The main objective of this research is to evaluate the effects of DEM resolution on landslide susceptibility modeling. For this purpose, statistical methods, including frequency ratio and certainty factor methods applied considering 30, 45, 60, 75, and 90m DEM resolutions. The accuracy of results of landslide susceptibility maps at different DEM resolutions was evaluated using the receiver operating characteristic curve (ROC), landslide density, and area under the curve (AUC) analysis. The resulted maps will use for landslide mitigation purposes and regional land use planning and will provide important information for researchers to choose the appropriate DEM resolution for landslide susceptibility mapping.

Study Area

The study area (Gundwin) covers approximately 323 km^2 in the northwestern highlands of Ethiopia, and lies between 37.9° E, 38.39° E longitude, 10.8° N, and 11.06° N latitude, which characterized by mountain peaks, deep gorge (valley), plateau and undulating topography with minimum and maximum altitudes of 1,198m and 3,199m, respectively (Fig. 1). Many tributaries are available in the entire study area and joined the Gonji and Tigidar River, which drains into the Abay River. The various streams in the study area caused the removal of soil through stream bank erosion. From field observation evidence, the study area is highly affected by gulley erosion, which also resulted in landslide incidences. The study area also

characterized by tropical (1,830m), subtropical (1,830 – 2,440m) and cool (> 2,440m) climate zones. Annual rainfall of the study area varies from 762 mm – 1,824 mm, which showed a pronounced seasonality with the heaviest rainfall being in July and August.

Materials And Methods

Materials

Data used

Relevant data including Advanced Spaceborn Thermal Emission and Reflection (ASTER) Digital Elevation Model (DEM) with 30 m resolution, historical landslide events, geological map, and meteorological data were collect (Table 1). These data were collected from Field Survey, Google Earth Imagery from the USGS website, Geological Survey of Ethiopia (GSE), United States Geological Survey (USGS), and Ethiopian National Meteorological Agency (Table 1). The landslides location of the study area was identified using detailed field surveys, historical records, and Google Earth imagery analysis. These are classified into training and testing landslide data sets. The training landslide data sets used for model preparation, whereas the testing landslide data sets are used for model prediction accuracy evaluation. Based on the data availability, the local environment condition, literature, field evaluation, and local people interview, eight landslides-driving factors were determined. Using ArcGIS 10.1, the landslide driving factor maps and landslide inventory maps were prepared. Drainage density, Distance to drainage, slope angle, slope aspect, and curvature were derived from 30 m and resampled 45, 60, 75, and 90m resolution of Digital Elevation Model (DEM). The lithological layer digitized from the existing geological map of the Debre Markos sheet at a scale of 1:250,000. The land use map of the study area was prepared using ERDAS, ArcGIS, Sentinel 2 image, and Google Earth Imagery analysis.

Table 1 Table Information source for the various landslides factors used in the landslides susceptibility mapping

Data	Map	Format	Source
Landslide Inventory	Landslide Inventory Map	Vector (shapefile)	Google Earth Imagery, Field Survey and Historical record
Geology	Lithology Map	Vector (shapefile)	Digitized from Geological map of Debre Markos Sheet provided by the Geological Survey of Ethiopia at 1:50,000
Digital Elevation Model (DEM)	Slope Angle Map	Raster (grid)	Derived from 30 m DEM, using ArcGIS 10.1, Downloaded from USGS
	Aspect Map		
	Curvature Map		
Hydrology	Distance to Stream	Raster (grid)	Developed from DEM and buffering using distance to Euclidian and line density
	Stream Density		
Meteorological data	------	Vector (shapefile)	Ethiopian National Meteorological Agency
Land use	Land use Map	Vector (shapefile)	Sentinel 2 image in the USGS, Field Survey and Google Earth Imagery

Landslide Inventory

In landslide susceptibility mapping, landslide inventory mapping is one of the key elements to study the spatial relationship between landslide and landslide governing factors. The accuracy of landslide inventory data can influence the results of landslide susceptibility mapping. Landslide inventory data can be prepared using various techniques like the aerial photograph or Google Earth Imagery interpretation, field investigation, and evaluation of archived data coupled with GIS tools (Van Westen et al. 2008). Landslide inventory map used as the base for future landslide prediction by evaluating the relationship between the existing landslide event and landslide driving factors (Mohammad et al. 2011; Yalcin et al. 2011; Corominas et al. 2014). Van Westen et al (2000) prepared a landslide inventory map using GIS from field investigation, historical landslide events, and satellite image analysis. Landslide inventory maps can be also prepared using field surveys and Google Earth Imagery (Meten et al. 2015; Roy and Saha 2019; Zine et al. 2019; Wubalem and Meten 2020). In this study, from active and old landslide scarps, 894 landslides were identified using detailed fieldwork, historical landslide record, and time series Google Earth Imagery analysis. It digitized into polygons using a GIS tool with the help of Google Earth Imagery; finally, a landslide inventory map produced and stored in a geodatabase. From local people's

witness and time series Google Earth Imagery analysis, the study area was frequently affected by landslide incidence due to heavy and prolonged rainfall and the presence of unconsolidated soil deposits as well as highly weathered basalt rock unit. Debris flow, earth flow, earthfall, weathered rockslide, and Soil slide types of landslides are dominant in the study area. In literature, most of the researchers' classified landslides into 70% for training data sets and 30% for testing landslide data sets (Meten et al. 2015; Haoyuan et al. 2016; Anis et al. 2019; Qiqing et al. 2019; Roy and Saha 2019; Zine et al. 2019). Using ArcGIS 10.1, these landslides classified randomly into 70% (626) for training landslide data sets and 30% (268) for validation data sets keeping their spatial distribution. In landslide susceptibility mapping, evaluating the size and distribution of landslides is very important to use an appropriate DEM resolution. As a result, statistical analysis was performed to determine the distribution and the size of the landslide (Fig. 2). The analysis of observed landslides in the study area showed that the area of the largest landslide is 161,502.2 m^2, the smallest is 130.2 m^2, the average is 5,731.9 m^2, and the standard deviation is12, 133.5 m^2. As the result showed, 75% of landslide areas are covered by large landslides.

Landslide Factors

The select of landslide governing factors to use as input parameters in the landslide susceptibility model is one of the most important steps, besides, DEM resolution selection and landslide inventory mapping. In this research, the eight most significant landslide factors that can initiate the landslide incidence in the study area have been selected based on the data availability, statistical analysis, local environmental conditions, literature review, local person interview, and field evaluation. These are distance to drainage, drainage density, rainfall, land use, slope angle, aspect, curvature, and lithology. They are taken into account to examine the spatial relationship between them and landslide occurrence in the study area. Distance to drainage (five classes), drainage density (seven classes), slope angle (five classes), aspect (ten classes), and curvature (three classes) maps were constructed (Fig. 3) for each of 30, 45, 60, 75, and 90 m resolution Digital Elevation Model (DEM). After downloading the 30 m resolution and the remaining DEM resolutions (45, 60, 75, and 90 m) derived by resampled 30 m resolution. The lithological map of the study area was prepared through digitization from 1:250,000 existing geological maps of Debre Markos sheet from the Geological Survey of Ethiopia, which has five classes (highly weathered basalt, slightly weathered basalt, alluvial soil, residual soil, and colluvial sediments). The land use map of the study area was prepared by digitized from Google Earth Imagery, and the supervised classification of Sentinel 2 images. The earthquake is not considered in the present work because the study area is so far from the active Earthquake sites. Table 1 shows, the source of various landslide factors used in landslide susceptibility mapping.

Slope angle is one of the most important factors in slope stability analysis which is directly related to the effects of gravity i.e. the shear stresses acting on the displacement of hill slopes (Bui et al. 2017). In this research, the slope map reclassified into five classes (<7°, 7°-15°, 15°-25°, 25°-36°, 36°-74°). The direction

of the slope and controls the variation of slope morphology and hydrology which in turn indirectly affects the slope stability condition is the characteristics of slope aspect (Meten et al. 2015; Ilia and Tsangaratons 2016; Nicu and Asandulesei 2018; Zhou et al. 2020). As indicated in Fig. 3, the slope aspect reclassified into 10 classes (flat (-1), north (0-22.5), northeast (22.5-67.5), east (67.5-112.5), southeast (112.5-157.5), south (157.5-202.5), southwest (202.5-247.5), west (247.5-292.5), northwest (292.5-337.5) and north (337.5-3600)) slope facing. Curvature is one of the landslides governing factors that measure the roughness of a given terrain. The curvature may refer to the convexness, concaveness, and flatness of a slope, which controls the hydraulic condition, and the effects of gravity for slope stability. In this research, the curvature map is reclassified into three classes (convex, concave, and relatively flat area). In the study area, landslides are common in concave and convex shaped slope. This is because of the hydraulic and gravity effect of concave and convex slopes. The concave upward slope enhanced rainwater impounding and infiltration into the soil mass. This further enhances the reduction of shear strength of soil mass in the slope. Land use and land cover is another key factor for landslide occurrence. The land use map of the study area encompasses seven classes including forest, woodland, cropland, bare land, grassland, waterbody, and scatters bush (Fig. 3). In the study area, landslides occurred in scattered woodland, bare land to scattered vegetation covers, and along stream/river banks. This confirms that land use/cover has a great role in slope instability. Distance to drainage and drainage density reflects the degree of river and surface incision of the given watershed. In the study area, landslide occurrence has a strong relation with distance to drainage (<200 m, 200-300 m, 300-400m, 400-500 m, 500-600 m and >600 m) and stream density (0-2.9, 2.9-5.8, 5.8-8.7, 8.7-11.5, 11.5-14.5, 14.5-18.2, and 18.2-27.3 Km/Km2). Therefore, in this research, distance to drainage and drainage density is very important landslide factors to use as input parameters in landslide susceptibility modeling. Lithology is one of the most commonly used input parameters for landslide susceptibility modeling because it can control the surficial process, hydrological and mechanical properties of the slope material. The lithology of the study area has five classes including colluvial deposit, highly weathered basalt, slightly weathered basalt, residual soil, and alluvial soil deposit (Fig. 3). Rainfall is one of the most important landslides triggering factors. As usual, slope failure will occur when shear stress in the slope exceeds the shear strength of slope material due to a change in rainfall pattern in a specified region. As rainwater infiltrates into the slope through soil or rock pores, the degree of saturation of soils or rocks will increase and the groundwater level will raise. This will also lead not only to an increase in pore water pressure and moisture content of the soil but also a decrease in effective stress in soil grains and reduce the shear strength of the slope material. As the moisture content increase in soil mass, the surface tension between particles and the intermolecular attractive force between soil particles will decrease. This causes the soil to behave as a fluid. This is again causing slope failure. Mostly, slope failure has occurred in the middle, end of July, August, and September with intense and prolonged rainfall in the study area. This shows that rainfall is one of the most important triggering factors for slope failure in the study area. However, rainfall effects depend on intensity, duration, soil depth, slope gradient, the rate of soil erosion, and anthropogenic activity. Although there is no adequate rain gage station in the study area, the rainfall data collected in various representative rain gage station and interpolated into 10 classes (610.5-729.9, 729.9-

826.1, 826.1-899.1, 899.1-958.7, 958.7-1,031.7, 1,031.7-1,117.9, 1,117.9-1,200.8. 1,200.8-1,283.7, 1,283.7-1,363.3, 1,363.3-1,456.2 mm) using IDW in the GIS spatial analysis tool.

Methods

For this research, data collection, Field investigation, landslide inventory mapping, Google Earth Imagery analysis, landslide factor evaluation, and mapping, GIS-based frequency ratio, and certainty factor LSM and validation were applied. Geodatabase building is one of the most fundamental elements in landslide susceptibility mapping. Thus, A set of ten geodatabases were built using Geographic Information System (GIS) for each DEM, eight landslide governing factors, and landslide inventory. These databases contained landslide inventory and landslide factors with the same projection (UTM) and pixel size. After the databases were built, an evaluation of the relationship between landslide and landslide factors as well as the determination of the statistical significance of each landslide factor is the next step in landslide susceptibility mapping. Then, eight landslide factor maps were reclassified into subclass and overlaid with reclassified training landslide data sets. Weight ratings for all landslide factor classes apportioned statistically using Excel as showed in Eq. (1, 3 & 4). These weighted maps rasterized-using lookup in spatial analyst. After rasterized the factor maps, the landslide susceptibility index maps generated by sum-up all raster maps using a raster calculator in Map Algebra. These maps (LSI) are classified into a fivefold classification scheme: very low, low, moderate, high, and very high susceptibility classes using natural breaks (Fig. 5 and 6). Finally, the accuracy of the models was evaluated using the prediction rate curve and landslide density based on observed testing landslide data sets.

Frequency Ratio Model

It is one of the bivariate probability methods, which is pertinent to determine the association between landslide occurrence and landslide causative factor classes. The frequency ratio (FR) is the ratio of areas where the landslide occurred in the areas of the landslide factor class to the areas where landslides not occurred. When the FR value is greater than one, it indicates the strong rapport between factor class and landslide occurrence in a given terrain, however, the ratio value less than one is indicated a weak relationship between landslide occurrence and landslide factors, which means a low probability of landslide occurrence (Bonham-Carter 1994; Lee and Talib 2005). It can be calculated using Eq. 1.

$$FR = \frac{a}{b} = \frac{\frac{Nslpix}{Ntslpix}}{\frac{Ncpix}{Ntcpix}} \qquad (1)$$

Where FR is frequency ratio, Nslpix is a landslide pixel/area in a landslide factor class, Ntslpix is the total area of a landslide in the entire study area (**a**), Ncpix is an area of the class in the study area and Ntcpix is the total pixel area in the entire study area (**b**). In the present research work, the frequency ratio for each causative factor class was calculated using Eq.1, and the results are summarized in Table 2.

After calculation of the frequency ratio for each landslide factor class using Microsoft Excel and GIS, the frequency ratio value for each factor class is assigned through the join in the ArcGIS tool. Then the weighted landslide factors were rasterized using the lookup tool in spatial analysis. The landslide susceptibility index indicated the degree of susceptibility of the area for landslide occurrence. The landslide susceptibility index (LSI) of the study area was calculated by carefully summing up the weighted rasterized factor raster maps using Eq. 2, by raster calculator in Map Algebra of the spatial analysis tool. To get the landslide susceptibility index, the frequency ratio of each factor type or class is summed as in Eq. 2.

$$LSI = \sum_{i=1}^{n} FR_i X_i \tag{2}$$

$$
\begin{aligned}
LSI = {} & FR * Slope\ raster + FR * Aspect\ raster + FR * Curvature\ raster + FR * Lithology\ raster \\
& + FR * Land\ use\ raster + FR * Distance\ to\ drainage\ raster + FR \\
& * Drainage\ density\ raster + FR * Rainfall\ raster
\end{aligned}
$$

Where LSI is the landslide susceptibility index, n is the number of landslide factors, X_i is the landslide factor and FR_i is the frequency ratio of each landslide factor type or class. After the landslide susceptibility index was calculated, the index values were classified into a different level of landslide susceptibility zones using natural breaks in the ArcGIS tool. The higher the value of the landslide susceptibility index (LSI), the higher the probability of landslide occurrence, but the lower the LSI indicating, the lower the probability of landslide occurrence.

Based on the natural break classification, the landslide susceptibility map of the study area has five classes such as very low, low, moderate, high, and very high landslide susceptibility class (Fig. 5).

Certainty Factor Model

The certainty factor is one of the probabilistic methods that widely used for landslide susceptibility mapping for different data (Kanungo et al. 2011; Sujatha et al. 2012; Pourghasemi et al. 2013c; Liu et al. 2014). Shortliffe and Buchanan (1975) proposed the certainty factor (the probability function) for landslide susceptibility mapping later Heckeman (1986) improved it and it expresses mathematically as:

$$
CF = \begin{cases}
\dfrac{PP_a - PP_b}{PP_a(1 - PP_b)} & if\ PP_a \geq PP_b \\[2ex]
\dfrac{PP_b - PP_b}{PP_b(1 - PP_a)} & if\ PP_a \leq PP_b
\end{cases} \tag{3}
$$

Where PP_a is the conditional probability of landslide in the defined area **a** and PP_b is the prior probability of landslide in the defined entire study area **b**. The CF value ranges from -1 to 1, a positive value indicates increasing certainty of landslide occurrence, and a negative value indicates decreasing of certainty of landslide occurrence. If the certainty value is close to zero, it means there is no adequate information about the relation between landslide factor classes and landslide occurrence; therefore, it is difficult to give any certainty of landslide occurrence (Sujantha et al. 2012; Dou et al. 2014).

The CF values were calculated for all landslide factor classes through overlaying landslide factors with landslides using Eq. 3 and Eq. 4. After the calculation of CF for each landslide factor class, the landslide susceptibility index (LSI) is determined as in Eq. 5.

$$Z = \begin{cases} X + Y - XYX, & Y \geq 0 \\ \dfrac{X+y}{1 - \min(|X|,|Y|)} & X * Y < 0 \\ X + Y + XYX, & Y < 0 \end{cases} \qquad (4)$$

Where Z is the calculated CF value, X and Y are two different layers of information.

$$LSI = \sum_{i=1}^{n} CF_i X_i \qquad (5)$$

$$LSI = CF * Slope\ raster + CF * Aspect\ raster + CF * Curvature\ raster + CF * Lithology\ raster +$$
$$CF * Land\ use\ raster + CF * Distance\ to\ drainage\ raster + CF * Drainage\ density\ raster +$$
$$CF * Rainfall\ raster$$

Where LSI is the landslide susceptibility index and CF_i is the certainty factor.

Landslide Susceptibility Map Validation

Evaluation of Landslide susceptibility map is a vital element in landslide prediction modeling, without validation, the landslide susceptibility maps will not have a grantee in the scientific world, and it is unusable (Wubalem and Meten 2020). Validation of the landslide susceptibility model is very essential to appraise the degree of precision of modeling using different validation techniques (Gorsevski et al 200; Chung and Fabbri 2003). For this purpose, the landslide area was classify based on time, space, and random partition (Chung and Fabri 2003, Lee and Pradhan 2007, and Meten et al. 2015). The landslides in the study area were classified into 70% (626) training landslide data sets and 30% (268) validation landslide data sets randomly keeping their spatial distribution. The value of the area under the curve (AUC) is used to appraise the performance of the model, and its value range from 0.5 – 1 (Yesilnacar and Topal 2005). When the AUC value in between the range of 0.9 – 1, the model has excellent performance;

if an AUC value in between the range of 0.8 − 0.9, the model has very good performance. If the AUC value between the range of 0.7 − 0.8, the model has good performance. If the AUC value between the range of 0.6 − 0.7, the model has an average performance. However, if AUC values between the range of 0.5 − 0.6 and equal to 0.5 or less than o.5, the model has poor performance (Yesilnacar and Topal 2005). The AUC contains a success rate curve and the prediction rate curve, which was calculate by overlaid landslide susceptibility map with training and validation landslide data sets. The success rate curve and prediction rate curve helps to evaluate the efficiency of the model and how well the model and landslide governing factors can predict landslide incidence, respectively. The accuracy of the models was also validated using the landslide densities in each of the landslide susceptibility classes. Landslide density is the ratio of percent of a landslide in a susceptibility class to the percent of susceptibility class which is calculated by overlaid validation landslide with landslide susceptibility map. As an increase in the value of landslide density with increase landslide susceptibility classes, the accuracy of the model becomes higher.

Results And Discussions

Results

In this section, the results of ten landslide susceptibility models which were generated at different DEM resolutions (30, 45, 60, 75 &90 m) using FR and CF statistical methods presented and compared.

Statistical Relationship of Landslide Factors and Past landslides

Using the frequency ratio (FR) and certainty factor (CF) methods, the statistical relationship between the landslide governing factors and the existing landslides was calculated through overlaid of landslides with landslide governing factors by ArcGIS tool. After calculated the FR and CF values of factor classes for each of five DEM resolutions (30, 45, 60, 75, and 90 m), the statistical significance of each factor class for landslide probability was analyzed (Fig. 4). When the FR value > 1, positive for CF, the factor class has a strong statistical correlation for landslide probability but if it is less than one, and negative for CF, the factor class shows a weak statistical correlation for landslide probability. In the case of slope angle and drainage density, the FR and CF values increased as the slope angle and drainage density increased, then the landslide occurrence probability increased (Fig. 4). The colluvial deposit and slightly weathered basalt are indicating a strong statistical correlation to landslide occurrence probability (Fig. 4). As indicated in Fig. 4, the aspect class of flat, N, SW, and W facing of the slope have higher statistical significance for landslide occurrence probability as the gully erosion, drainage density, and springs concentrated in these aspect classes. In the case of slope curvature, the concave and convex shaped slope class showed a strong statistical correlation for landslide occurrence probability (Fig. 4) due to the rainwater impounding effect and the effects of gravity, respectively. As indicated in Fig. 4, the land use/cover (bare land, scatter bush, woodland, and moderate forestland) has shown a strong statistical association for landslide occurrence probability. The first class of distance to drainage indicated a strong statistical association for landslide occurrence probability (Fig.4,), but as the distance increased the

effects of the river for landslide incidence decreased. The effects of rainfall depending on the intensity, duration of rainfall, the hydraulic behavior and depth of soil, slope gradient, the rate of soil erosion, and anthropogenic activity. As showed in Fig. 4, the rainfall class of 826.1-899.1 mm, 899.1-958.7 mm, and 958.7-1,031.7 mm) indicated a strong statistical association for landslide occurrence probability.

Landslide Susceptibility Models

To evaluate the effects of DEM resolution, each of the ten landslide susceptibility maps classified into five schemes of classification: Very low, low, moderate, high, and very high susceptibility classes (Fig. 5) using the natural break classification method. Fig. 5 &.6., indicated landslide susceptibility maps that produced using FR and CF considering five DEM resolutions, respectively. Regardless of the DEM resolution, the success rate curve and prediction rate curve values of AUC for the FR method is higher and showed very good performance to classify the region based on the degree of susceptibility of the area. As the results of susceptibility maps of each DEM resolution indicated in Fig. 7, the high and very high susceptibility area distribution and extent are more or less similar except the 45 and 90 m resolutions, which showed few differences. The high and very high susceptibility classes are mainly distributed in the fragile topography, middle and lower parts of the watershed area on non-vegetated area, dense stream network where many historical landslides were observed. Nevertheless, the low and very low susceptibility classes are mainly found in the flat and dense vegetation areas of upstream and water divider zones of the regions. From the factor class analysis of FR and CF models, the slope angle, distance to drainage, drainage density, land use, and lithology indicting higher landslide probability.

Area Under the Curve (AUC) Analysis

The landslide susceptibility maps of the study area endorsed employing training and testing/validation landslide data sets with the success rate curve and predictive rate curve. The success rate curves for the two models were calculated from the training landslide data sets through combining tools with landslide susceptibility classes, which were used to evaluate how well the models classified the region based on the existing landslide events (Meten et al. 2015; Silalahi et al. 2019). The prediction rate curve for the three models was calculated from the validation landslide datasets, which were used to evaluate how well the models can predict the unknown forthcoming landslide incidence (Mezughi et al. 2011; Silalahi et al. 2019).

Fig. 8, Showed the AUC values of ten susceptibility maps at different DEM resolution for validation and training landslides. Each of the curves displayed the values of AUC for the FR and CF statistical methods with corresponding DEM resolution (30, 45, 60, 75, and 90 m). As indicated in Fig. 8, the success rate

curves value of AUC for the FR model ranges from 81% – 85%, which fell in the range of very good performance for each of ten models at the different DEM resolution. Although the AUC values for the five DEM resolutions do not constant, the models classified the region very well. The AUC value of success rate curves for the CF model with five DEM resolutions range from 76-81%, which fell in the range of good to very good model performance. When someone wants to compare the model performance of the FR and CF statistical methods considering the results of five DEM resolution, the FR model showed a little bit better performance (Fig. 8). Fig. 8 showed the AUC value of prediction rate curves of FR and CF range from 81-92%, which fell in the range of very good to excellent prediction accuracy for five DEM resolutions. The AUC value for DEM resolution finer than 60 m except for some anomaly in 45 m, the results closely imitate, indicating higher model performance and higher prediction accuracy for FR and CF models. For DEM resolution coarser than 60 m, the result showed very sharp increments, indicating very good model performance and prediction accuracy. In general, the AUC value of prediction rate curves for the FR and CF models considering five DEM resolution is more or less the same, but it becomes peak when the DEM resolution coarser (75 and 90 m). For the study area, the maximum AUC value in the prediction rate curve was found in 90 m DEM resolution. The AUC values of prediction rate curves are slightly higher than the AUC values of success rate curves.

The clear analysis of the AUC values of the prediction rate and success rate curves displayed in Fig. 9. This denotes the variation of AUC values within five DEM resolution for the FR and CF statistical methods. These curves form an 'N' shape as DEM resolution becomes coarser, indicting coarser raster resolutions do necessarily lead to a better landslide susceptibility mapping than the finer resolutions when the larger landslide covers a relatively large area than the small landslides. Even though the optimum models appeared as the resolution decreased/ coarser, it is difficult to conclude in a wide range of landslide susceptibility evaluation. For the 45 DEM resolution, the AUC value showed an anomaly performance increase. Based on the AUC value of success rate and prediction rate curves, the FR model for 90 m resolution becomes better statistical methods for both capable to predict landslide occurrence and capable to classify stable and unstable regions at coarser resolutions. In addition to AUC analysis, the landslide density analysis was performed to evaluate the performance and prediction accuracy of the models. Fig 9 showed the relationship between landslide distribution and landslide susceptibility classes. The value of landslide density (LD) increased as the landslide susceptibility grade increased for the five DEM resolution of FR and CF statistical methods. In particular, the landslide density showed an anomaly increased at 45 m resolution and become a peak when we moved to the coarser DEM resolution (90 m) of FR and CF models. This again confirms that the landslide susceptibility model is better at coarser DEM resolution.

Discussion

Landslide susceptibility map is the results of the statistical association of landslide and landslide governing factors which cannot be anticipating not only when the landslides will occur but also the volume and rate of recurrence of the landslide, however, it can predicting where the landslides will occur in a region. Although the landslide susceptibility maps have limitations to predict the time and the volume of future landslide occurrence, it is very important to get the spatial distribution of landslide-prone areas in a given terrain. Therefore, decision-makers can use the map for regional land use planning, landslide hazard mitigation, and prevention purposes (Fell et al. 2008; Oh et al. 2009; Yilmaz and Kskin 2009; Mezughi et al. 2011; Das and Lgcha 2019; Mandal and Mondal 2019; Silalahi et al. 2019). However, the performance of these predictive models of landslide susceptibility highly depends on the quality of the input parameters. Therefore, it is very important to evaluate the quality of the input parameters before use as input in the predictive modeling of landslide susceptibility. For example, DEM resolution can affect the quality of the predictive landslide model that depending on the average sizes of landslides in the area. This is because the details of the morphometric information provided from the DEM (slope, aspect, curvature) depends upon its spatial resolution (Paudel et al. 2016). In this study, the scale effects of the morphometric (slope, aspect, curvature, distance to drainage, and drainage density) factors derived from 30 m and resampled 45, 60, 75, and 90 m DEM resolutions were analyzed. After analyzing the statistical association of landslide governing factors and preexisting landslides in the region using FR and CF methods under considering five DEM resolutions (30, 45, 60, 75, and 90 m), the landslide susceptibility maps of the study area were generated with five class of very low, low, moderate, high and very high susceptibility classes using natural break method. The resulted maps were compared for each of 30, 45, 60, 75 and 90 m DEM resolutions using receiver operating characteristics curve (ROC), area under the curve (AUC) of success rate, and predictive rate curves, and landslide density. As the outcomes indicated in Fig.8, the success rate and predictive rate curve values of AUC become maximum when the DEM resolution becomes coarser (90 m resolution). These results are similar to the early studies, which show that the coarser DEM resolutions (70 m) did necessarily yield the best performance of landslide susceptibility appraisal of a specific region (Palamakumbure et al. 2015; Mahalingam and Olson 2016; Mahalingam et al. 2016; Cama et al. 2016; Pradhan and Sameen 2017; Zhou et al. 2020). This important finding may be linked to the size of landslides that have occurred in the study area (Zhou et al. 2020). As designated in Fig.2, the frequency of the small landslides is more than the frequency of larger landslides; however, the areas covered by the larger landslides are more than the frequently occurred small landslides. As shown in Fig. 2, more than 25% cumulative percent of landslides are covered by the larger landslides, but only 24.5% are small landslides. As a result, the model performance and prediction accuracy increased when the DEM resolutions become coarser in this case 90 m (Zhou et al. 2020). Therefore, this finding may serve as a base for researchers to choose the appropriate DEM resolution before landslide susceptibility mapping. The precision of the landslide susceptibility map highly depends on the DEM resolution, landslide governing factor selection, and the accuracy of the landslide inventory mapping. For example, the use of fine DEM resolution allows us to capture more detailed morphometric features (Dietrich and Montgomery 1998) of small, shallow landslides (Penna et al. 2014; Ciampalini et al. 2016; Reichenbach et al. 2018; Zhou et al. 2020). Nevertheless, fine DEM resolution may not have a strong statistical correlation for landslide susceptibility analysis of large to very large, deep-seated

landslides whose morphometric is appropriate for coarser DEM resolutions (Lee et al. 2010; Reichenbach et al. 2018; Zhou et al. 2020). Therefore, it is desirable to use coarser DEM resolution to landslide susceptibility mapping where the size of landslides is relatively large by resampling fine DEM resolution.

There is some literature regarding the comparison of prediction accuracy of the certainty factor method with the frequency ratio method. From the work of Haoyuan et al (2016), based on the predictive rate value of the area under the receiver operating characteristic curve (AUC), the frequency ratio and certainty factor models showed more or less similar predictive capacity, which is 81.18% for the certainty factor model and 80.14% for the frequency ratio model. However, CF has shown a bit of little performance than the Frequency ratio model. In the work of (Wubalem 2020), the two models showed an almost similar AUC value of the prediction rate curve (87.03% for the certainty factor model and 88.8% for the frequency ratio model). Similarly in the present study, although the range of the predictive rate values for five DEM resolution (30, 45, 60, 75, and 90 m) fell in the same range of accuracy, the frequency ratio method showed a bit better performance (AUC=86-92%) than the certainty factor method with predictive rate value of AUC= 81-89%. Generally, the two bivariate statistical methods in literature and this study showed, the closer prediction capacity with AUC >80%, respectively fell in the range of very good performance (Yesilnacar and Topal 2005). In this study, the landslide validation results for two statistical methods are more or less closer to each other and it fell in the same range of very good performance. Besides this, the density of landslides for all DEM resolution shows an increased value from very low to very high susceptibility classes for FR and CF statistical methods (Fig. 9b). Therefore, from these results, the research work finds out that in landslide susceptibility mapping, the two models have equal potential to generate landslide-prone areas but DEM resolution selection, factor selection, and landslide inventory mapping required attention than statistical methods.

Conclusion

 Landslide susceptibility mapping is a very essential element in environmental management and to reduce damages due to natural hazards. However, the precision of this map is highly sensitive for DEM resolution, factors, and the accuracy of landslide inventory data. An appropriate DEM resolution will provide reliable and accurate results. In this study, various DEM resolutions using frequency ratio and certainty factor statistical methods were used to landslide susceptibility assessment. The results showed that the landslide susceptibility map produced from the 90 m DEM resolution is the most statistically significant. From this result, the conclusion can be drafted as using the finest resolution (in this case 30 m) does not always assure the best predictive accuracy. This agrees with the prior studies (Palamakumbure et al. 2015; Mahalingam and Olson.2016; Mahalingam et al. 2016; Cama et al. 2016; Pradhan and Sameen 2017; Zhou et al. 2020). In this study, although the range of the predictive rate values for five DEM resolution (30, 45, 60, 75, and 90 m) fell in the same range of accuracy, the frequency ratio method showed a bit better performance (AUC=86-92%) than the certainty factor method with predictive rate value of AUC= 81-89%.

Declarations

Authors' Contributions

All activities starting from the conception and design of the work, the developments of the models as well as the statistical analysis and interpretations of the results were done by me.

Funding

It is not applicable in this case.

Availability of data and material

All the datasets that have been used and analyzed during the current study are available from the corresponding author on reasonable request.

Competing interests

I have declared that there are no competing interests.

Author details'

Department of Geology, University of Gondar, Ethiopia

References

Akgu¨n A, Dag S, Bulut F (2008) Landslide susceptibility mapping for a landslide-prone area (Findikli, NE of Turkey) by likelihood-frequency ratio and weighted linear combination models. Environ Geol 54:1127–1143

Aleotti P., and R. Chowdhury (1999) Landslide hazard assessment: summary review and new perspectives. Bulletin of Engineering Geology and Environment 58: 21–44

Anis Zorgati*, Gallala Wissem, Vakhshoori Vali, Habib Smida, and Gaied Mohamed Essghaiem (2019)GIS-based landslide susceptibility mapping using bivariate statistical methods. OpenGeosci 11:708–726

Bednarik M, Yilmaz I, Marschalko M (2012) Landslide hazard and risk assessment: a case study from the Hlohovec–Sered' landslide area in south-west Slovakia. Nat Hazards DOI:10.1007/s11069-012-0257-7

Bonham-Carter GF (1994) Geographic information systems for geoscientists. Modeling with GIS. Pergamon, Oxford 398

Cama M, Conoscenti C, Lombardo L, Rotigliano E (2016) Exploring relationships between grid cell size and accuracy for debris-flow susceptibility models: a test in the Giampilieri catchment Sicily, Italy. Environ

Earth Sci 753:238

Catani F, Lagomarsino D, Segoni S, Tofani V (2013) Landslide susceptibility estimation by random forests technique: sensitivity and scaling issues. Nat Hazard Earth Syst 1311:2815–2831

Ciampalini A, Raspini F, Frodella W, Bardi F, Bianchini S, Moretti S (2016) The effectiveness of high-resolution LiDAR data combined with PSInSAR data in landslide study. Landslides 132:399–410

Chandak P.G., Sayyed, S.S., Kulkarni, Y.U., Devtale, M.K (2016) Landslide hazard zonation mapping using information value method near Parphi village in Garhwal Himalaya. Ljemas 4: 228 – 236

Bui DT, Tuan TA, Hoang ND, Thanh NQ, Nguyen DB, Van Liem N, Pradhan B (2017) Spatial prediction of rainfall-induced landslides for the Lao Cai area Vietnam using a hybrid intelligent approach of least squares support vector machines inference model and artificial bee colony optimization. Landslides 142:447–458

Brunsden, D (1979) Mass movement. In: C. Embleton and J. Thornes (eds.), Processes in Geomorphology, Edward Arnold Ltd, London, UK 436

Chen, Z., and Wang, J (2007) Landslide hazard mapping using a logistic regression model in Mackenzie Valley, Canada. Nat. Hazard 42(1) : 75-89

Chung CJ, Fabbri AG (2005) Systematic procedures of landslide hazard mapping for risk assessment using spatial prediction models. In: Glade T, Anderson MG, Crozier MJ (eds) Landslide hazard and risk. Wiley, New York 139–177

Chung CJF., Fabbri AG (2003) Validation of Spatial Prediction Models for Landslide Hazard Mapping. Natural Hazards 30(3): 451-472

Corominas J, Van Westen C, Frattini P, et al (2014) Recommendations or the quantitative analysis of landslide risk. Bulletin of engineering geology and the environment 73:209-63

Cruden, D.M (1991) A simple definition of a landslide. Bulletin of Engineering Geology and Environment 43 (1): 27–29

Dai F. C. and Lee C. F (2002) Landslide characteristics and slope instability modeling using GIS, Lantau Island, Hong Kong. Geomorphology 42: 213-228

Das G, Lepcha K (2019) Application of logistic regression (LR) and frequency ratio (FR) models for landslide susceptibility mapping in Relli Khola river basin of Darjeeling Himalaya. India. SN Appl Sci 1:1453. HTTP ://doi.org/10.1007/s4245 2-019-1499-8

Dietrich WE, Montgomery DR (1998) SHALSTAB: a digital terrain model for mapping shallow landslide potential. NCASI National Council of the Paper Industry for Air and Stream Improvement Technical Report

1998

Donati L, and Turrini, M. C (2002) An objective method to rank the importance of the factors predisposing to landslides with the GIS methodology: application to an area of the Apennines (Valnerina; Perugia, Italy). Engg. Geol 63: 277-289

Dou J, Oguchi T, Hayakawa Y S, Uchiyama S, Saito H and Paudel U (2014) GIS-based landslide susceptibility mapping using a certainty factor model and its validation in the Chuetsu area, central Japan; In Landslide Science for a Safer Geoenvironment (Springer International Publishing) 419–424

Duman T.Y., Can, T., Gokceoglu, C., Nefesliogocu, H. A., and Sonmez, H (2006) Application of logistic regression for landslide susceptibility zoning of Cekmee area, Istanbul, Turkey. Verlag 242 – 256

 El Jazouli, Ahmed Barakat* and Rida Khellouk (2019) GIS-multicriteria evaluation using AHP for landslide susceptibility mapping in Oum Er Rbia high basin (Morocco)

Fell R, Corominas J, Bonnard C, Cascini L, Leroi E, Savage WZ (2008) Guidelines for landslide susceptibility, hazard, and risk zoning for land-use planning, joint technical committee (JTC-1) on landslides and engineered slopes. Eng Geol 102: 85–98

Gorsevski P V, Gessler P and Foltz R B (2000) Spatial prediction of landslide hazard using discriminant analysis and GIS; In GIS in the Rockies 2000 Conference and Workshop.

Gutiérrez F., R. Linares C. Roqué, M. Zarroca, D. Carbonel J. Rosell, and M. Gutiérrez (2015) Large landslides associated with a diapiric fold in Canelles reservoir (Spanish Pyrenees): Detailed geological–geomorphological mapping, trenching and electrical resistivity imaging. Geomorphology 241: 224–242

Haoyuan Hong, Wei Chen, Chong Xu, Ahmed M. Youssef, Biswajeet Pradhan & Dieu Tien Bui (2016) Rainfall-induced landslide susceptibility assessment at the Chongren area (China) using frequency ratio, certainty factor, and index of entropy. Geocarto International, DOI: 10.1080/10106049.2015.1130086

Heckeman (1986) Probabilistic interpretation of MYCIN's certainty factors; In Uncertainty in artificial intelligence (eds) Kanal L N and Lemmer J F (New York: Elsevier) 298–311

Ibrahim J (2011) Landslide assessment and hazard zonation in Mersa and Wurgessa, North Wollo, Ethiopia. Unpublished Master Thesis, School of Graduate Studies, Addis Ababa University, Addis Ababa, Ethiopia 1-10

Jagabandhu Roy and Sunil Saha (2019) Landslide susceptibility mapping using knowledge-driven statistical models in Darjeeling District, West Bengal, India. Geoenvironmental Disasters 6:11

Jia N, Xie M, Mitani Y, Ikemi H, Djamaluddin I (2010) A GIS-based spatial data processing system for slope monitoring. Int Geoinf Res Dev J 1(4)

Kanungo D P, Sarkar S, and Sharma S (2011) Combining neural network with fuzzy, certainty factor south-facing, and likelihood ratio concepts for spatial prediction of landslides; Nat. Hazards 59(3): 1491–1512

Kanungo D.P., Arora M.K., Sarkar S, Gupta R.P (2009) Landslide susceptibility zonation mapping a review. J South Asia Disaster stud 2: 81 – 105

Karimi Nasab S, Ranjbar H, Akbar S (2010) Susceptibility assessment of the terrain for slope failure using remote sensing and GIS, a case study of Maskoon area, Iran. Int Geoinf Res Dev J 1(3)

Kifle Woldearegay (2008) Characteristics of a large-scale landslide triggered by heavy rainfall in Tarmaber area, central highlands of Ethiopia Geophysical Research Abstracts 10

Kifle Woldearegay (2013) Review of the occurrences and influencing factors of landslides in the highlands of Ethiopia with implications for infrastructural development.

Kouhpeima S. Feizniab H. Ahmadib and Moghadamniab A.R (2017) Landslide susceptibility mapping using logistic regression analysis in Latyan catchment. Desert 85 – 95

Lee MF, Wang SF, Lin TC (2010) The effect of spatial resolution on landslide mapping—a case study in Chi-Shan river basin, Taiwan. In: 31st Asian conference on remote sensing 2010 (ACRS 2010)

Lee S, Choi J, Woo I (2004) The effect of spatial resolution on the accuracy of landslide susceptibility mapping: a case study in Boun. Korea Geosci J 8(1):51

Li J, Zhou CH (2003) Appropriate grid size for terrain-based landslide risk assessment in Lantau Island, Hong Kong. J Remote Sens Beijing 7(2):86–92

Lee S, Pradhan B (2007) Landslide hazard mapping at Selangor, Malaysia using frequency ratio and logistic regression models, Landslides 4:33–41

Lee S, Pradhan B (2006) Probabilistic landslide hazards and risk mapping on Penang Island, Malaysia. J Earth Sys Sci 115(6):661–667

Lee S, Talib JA (2005) Probabilistic landslide susceptibility and factor effect analysis. J Environ Geol 47:982–990

Liu M, Chen X and Yang S (2014) Collapse landslide and mudslide hazard zonation; In Landslide science for a safer geoenvironmental (Springer International Publishing) 457–462

Luelseged Ayalew and Yamagishi H. (2005) the application of GIS-based logistic regression for landslide susceptibility mapping in the Kakuda- Yahiko Mountains, Central Japan. Geomorphology 65:15 – 31

Luelseged, Ayalew (1999) the effects of the seasonal rainfall on a landslide in the highland of Ethiopia. Bull Engineering Geology and Environment 58: 9-19

Meten, M., Bhandary, N.P., and Yatabe, R. (2015) GIS-based frequency ratio and logistic regression modeling for landslide susceptibility mapping of Debre Sina area in central Ethiopia. J.Mt.Sci 12(6): 1355 – 1372

Mezughi TH, Akhir JM, Rafek AG, Abdullah I (2011) Landslide susceptibility assessment using frequency ratio model applied to an area along the E-W Highway (Gerik-Jeli). Am J Environ Sci 7:43–50

Mahalingam R, Olsen MJ (2016) Evaluation of the influence of source and spatial resolution of DEMs on derivative products used in landslide mapping. Geomat Nat Haz Risk 7(6):1835–1855

Mahalingam R, Olsen MJ, O'Banion MS (2016) Evaluation of landslide susceptibility mapping techniques using lidar-derived conditioning factors, Oregon case study. Geomat Nat Haz Risk 7(6):1884–1907

Mandal S, Mondal S (2019) Probabilistic approaches and landslide susceptibility. Geoinformatics and modeling of landslide susceptibility and risk. Environmental science and engineering. Springer book series (ESE) 145–163

Mohammad M, Pourghasemi HR, Pradhan B. (2012) Landslide susceptibility mapping at Golestan Province, Iran: a comparison between frequency ratio, Dempster–Shafer, and weights-of evidence models. Journal of Asian Earth Sciences 61:22136

Oh HJ, Lee S, Wisut C, Kim CH, Kwon JH (2009) Predictive landslide susceptibility mapping using spatial information in the Pechabun Area of Thailand. Environ Geol 57:641–651

 Paudel U., Oguchi T. & Hayakawa, Y. Multi-Resolution (2016) Landslide Susceptibility Analysis Using a DEM and Random Forest. Int. J. Geosci 07: 726–743

Palamakumbure D, Flentje P, Stirling D (2015) Consideration of optimal pixel resolution in deriving landslide susceptibility zoning within the Sydney Basin, New South Wales, Australia. Comput Geosci UK 82:13–22

Penna D, Borga M, Aronica GT, Brigandì G, Tarolli P (2014) The influence of grid resolution on the prediction of natural and road-related shallow landslides. Hydrol Earth Syst Sci 18(6):2127–2139

Pradhan B, Sameen MI (2017) Effects of the spatial resolution of digital elevation models and their products on landslide susceptibility mapping. In: Laser scanning applications in landslide assessment 133–150

Park N-W. (2011) Application of Dempster-Shafer theory of evidence to GIS-based landslide susceptibility analysis. Environmental Earth Sciences 62:367-76.

Pourghasemi H R, Pradhan B, Gokceoglu C, Mohammadi M Moradi H R (2013c) Application of weights-of-evidence and certainty factor models and their comparison in landslide susceptibility mapping at Haraz watershed, Iran; Arabian J. Geosci 6(7): 2351–2365

Pourghasemi HR, Pradhan B, Gokceoglu C, Mohammadi M, Moradi HR (2012a) Application of weights-of-evidence and certainty factor models and their comparison in landslide susceptibility mapping at Haraz watershed, Iran. Arab J Geosci. DOI:10.1007/s12517-012-0532-7

Pradhan B, Chaudhari A, Adinarayana J, Buchroithner MF (2012) Soil erosion assessment and its correlation with landslide events using remote sensing data and GIS: a case study at Penang Island, Malaysia. Environ Monit Assess 184(2):715–727

Pradhan B, Lee S, Buchroithner MF (2010c) Remote sensing and GIS-based landslide susceptibility analysis and its cross-validation in three test areas using a frequency ratio model. Photogramm Fernerkun 1:17–32. DOI:10.1127/14328364/2010/0037

Pradhan B, Mansor S, Pirasteh S, Buchroithner M (2011) Landslide hazard and risk analyses at a landslide-prone catchment area using the statistical-based geospatial model. Int J Remote Sens 32(14): 4075–4087. DOI:10.1080/01431161.2010.484433

Qiqing Wang, Yinghai Guo, Wenping Li, Jianghui He & Zhiyong Wu (2019) Predictive modeling of landslide hazards in Wen County, northwestern China based on information value, weights-of-evidence, and certainty factor, Geomatics, Natural Hazards and Risk 10:1, 820-835, DOI: 10.1080/19475705.2018.1549111

Rai, P.K., K. Mohan, and V.K. Kumra (2014) Landslide hazard and its mapping using remote sensing and GIS. Journal of Scientific Research 58: 1–13

Regmi A. D., Yoshida K., Pourghasemi H. R., Dhital M. R., and Pradhan B. (2014) Landslide susceptibility mapping along Bhalubang-Shiwapur area of mid-western Nepal using frequency ratio and conditional probability models. Jour. Mountain Sci 11(5): 1266-1285

Saha AK, Gupta RP, Sarkar I, Arora KM, Csaplovics E (2005) An approach for GIS-based statistical landslide susceptibility zonation with a case study in the Himalayas. Landslides 2(1):61–69

Sarkar S., Kanungo D, Ptra A., Kumar P (2006) Disaster mitigation of debris flow, slope failure, and landslides. GIS-based landslide susceptibility case study in Indian Himalaya. Universal Acadamy Press, Tokyo, Japan 617 – 624

Sarkar S., Rjan Martha T., and Roy A. (2013) Landslide susceptibility Assessment using information value method in parts of the Darjeeling Himalayas. Geological Society of India 82: 351 – 362

Schlögel R, Marchesini I, Alvioli M, Reichenbach P, Rossi M, Malet JP (2018) Optimizing landslide susceptibility zonation: Effects of DEM spatial resolution and slope unit delineation on logistic regression models. Geomorphology 301:10–20

Shortliffe EH and Buchanan B G (1975) A model of inexact reasoning in medicine; Math. Biosci 23(3): 351–379

Silalahi, Florence Elfriede Sinthauli *, Pamela, Yukni Arifianti, and Fahrul Hidayat (2019) Landslide susceptibility assessment using frequency ratio model in Bogor, West Java, Indonesia. Geosci. Lett 6:10

Sujatha E R, Rajamanickam G V and Kumaravel P (2012) Landslide susceptibility analysis using probabilistic certainty factor approach: A case study on Tevankarai stream watershed, India; J. Earth Syst. Sci 121(5): 1337–1350

Sun W F (2009) Study of landslide hazard assessment on typical loess area in Qianhe valley, Qianyang County (Ph.D. dissertation: Chinese Academy of Geological Science

Tarolli P, Tarboton DG (2006) A new method for determination of most likely landslide initiation points and the evaluation of digital terrain model scale in terrain stability mapping. Hydrol Earth Syst Sci 10(5):663–677

Temesgen B., Mohammed U, Korme T (2001) Natural hazard assessment using GIS and remote sensing methods, with particular reference to the Landslides in the Wondogenet Area, Ethiopia. Physics and Chemistry of the Earth Part C: Solar Terrestrials & Planetary Science (C) 26: 665-615

Tian Y, Xiao C, Liu Y, Wu L (2008) Effects of raster resolution on landslide susceptibility mapping: a case study of Shenzhen. Sci China Ser E 51(2):188–198

Van Westen CJ, Castellanos E, Kuriakose SL (2008) spatial data for landslide susceptibility, hazard, and vulnerability assessment: an overview. Engineering geology 102:112-31

Varnes D. J (1984) Landslide hazard zonation, a review of principles and practice, International Association of Engineering Geology Commission on Landslides and Other Mass Movements on Slopes, UNESCO, Paris 63.

Wang HB, Wu SR, Shi JS, Li B (2011) Qualitative hazard and risk assessment of landslides: a practical framework for a case study in China. Nat Hazards DOI:10.1007/s11069-011-0008-1

Wubalem A.*, Meten M (2020) Landslide susceptibility mapping using information value and logistic regression models in Goncha Siso Eneses area, northwestern Ethiopia. SN Applied Sciences, Switzerland AG 2:807 | https://doi.org/10.1007/s42452-020-2563-0

Wubalem A (2020) Modeling of Landslide susceptibility in a part of Abay Basin, northwestern Ethiopia. Open Geosciences, Degruyter 12:1-28. https://doi.org/10.1515/geo-2020-0206

Yalcin A, Reis S, Aydinoglu A, Yomralioglu T (2011) AGIS-based comparative study of frequency ratio, analytical hierarchy process, bivariate statistics, and logistics regression methods for landslide susceptibility mapping in Trabzon, NE Turkey. Catena 85:274-87

Yesilnacar E, Topal T (2005) Landslide susceptibility mapping: A comparison of logistic regression and neural networks method in a medium scale study, Hendek region (Turkey). Engineering Geology 79: 251 –

Yilmaz I, Keskin I (2009) GIS-based statistical and physical approaches to landslide susceptibility mapping (Sebinkarahisar, Turkey). Bull Eng Geol Environ 68:459–471

Zine El Abidine, R., Abdel Mansour, N (2019) Landslide susceptibility mapping using information value and frequency ratio for the Arzew sector (Northwestern of Algeria). Bulletin of the Mineral Research and Exploration, 160:197-211. https://doi. org/10.19111/bulletinofmre.502343

Zhuo Chen1 · Fei Ye1 · Wenxi Fu1 · Yutian Ke · Haoyuan Hong (2020) The influence of DEM spatial resolu on landslide susceptibility mapping in the Baxie River basin, NW China. Natural Hazards, 25.

Figures
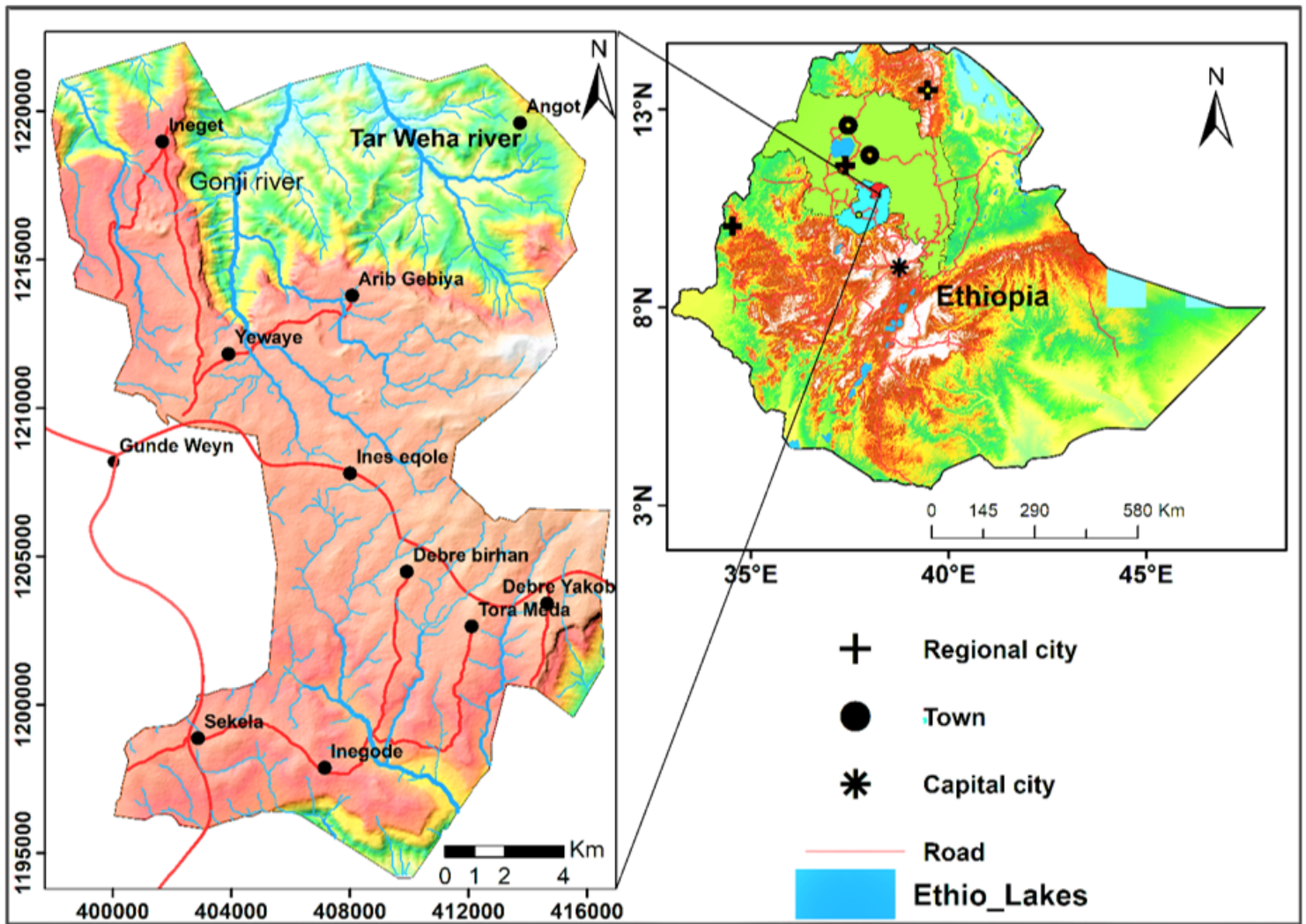
Figure 1

Location Map of the Study Area
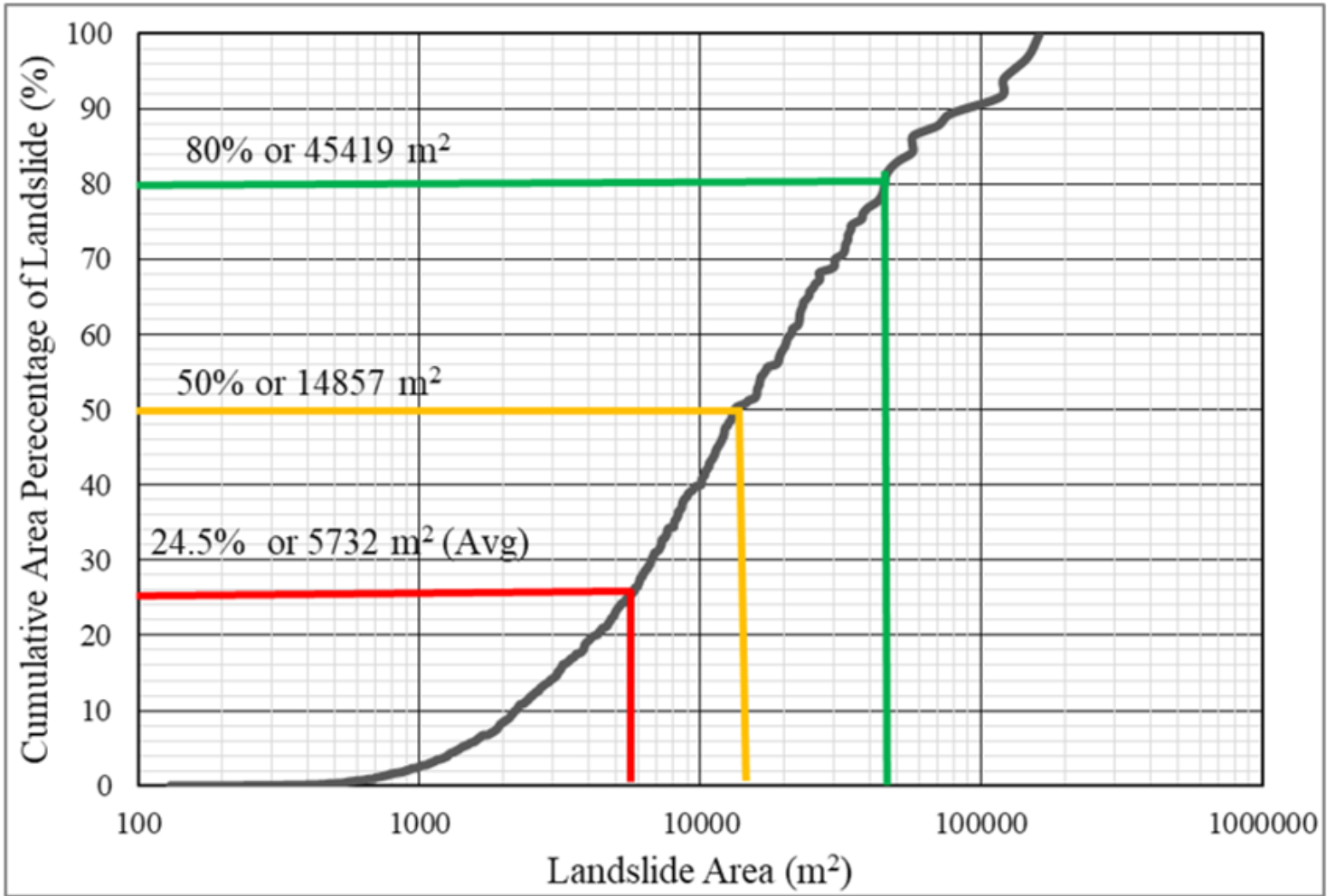
Figure 2

landslide size and distribution
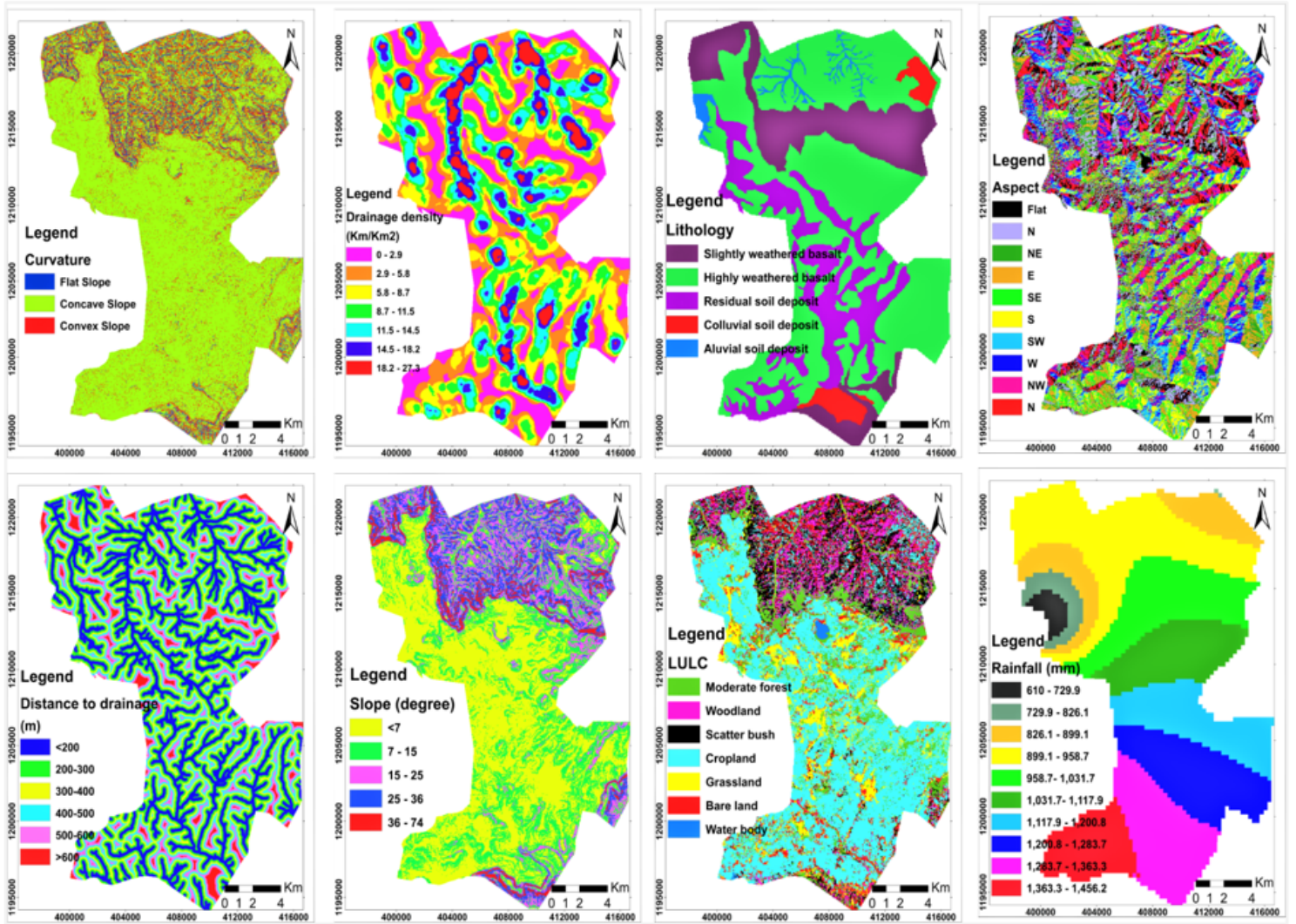
Figure 3

landslide governing factor maps of the study area
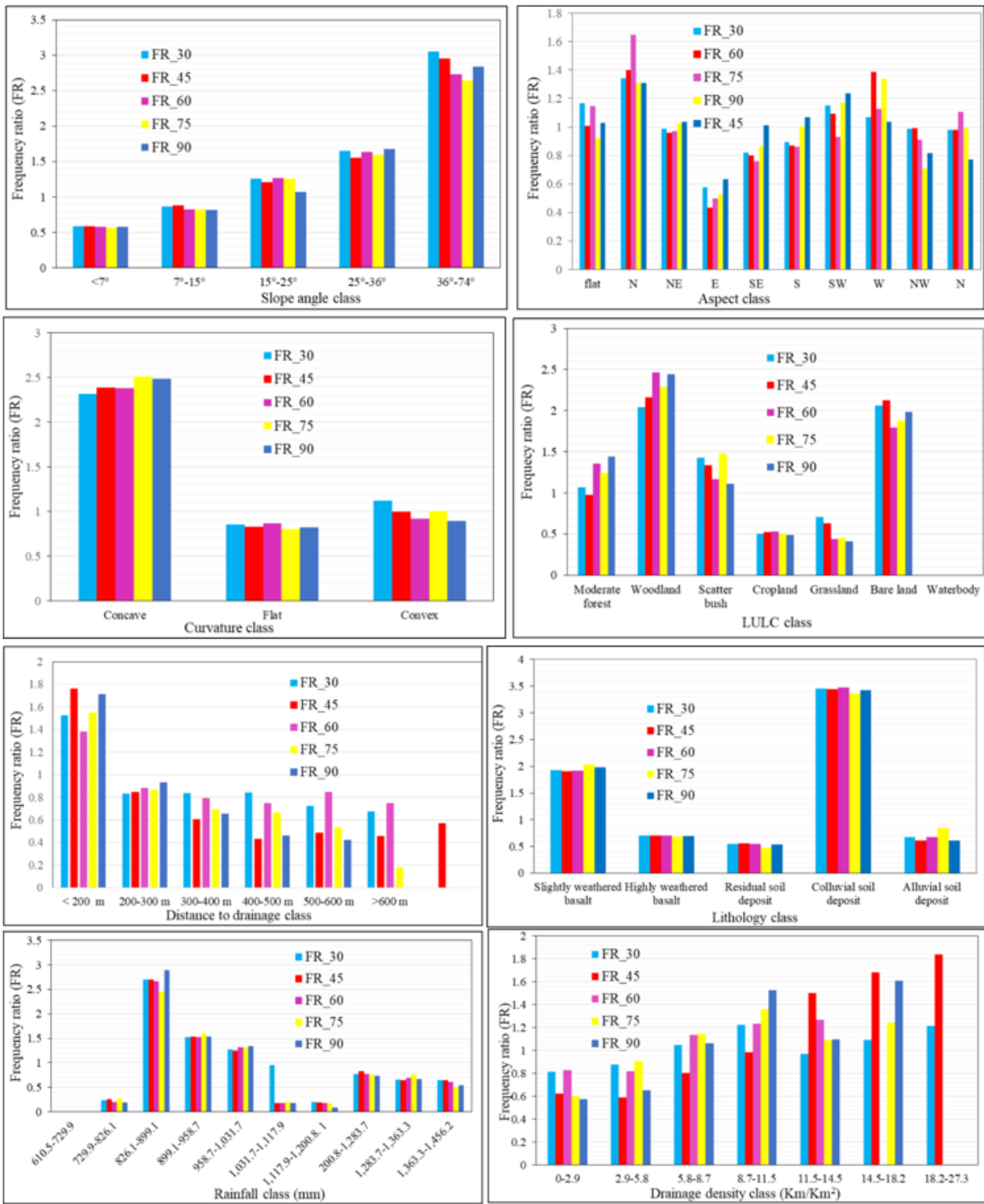
Figure 4

the statistical relationship between landslide governing factor classes and past landslides
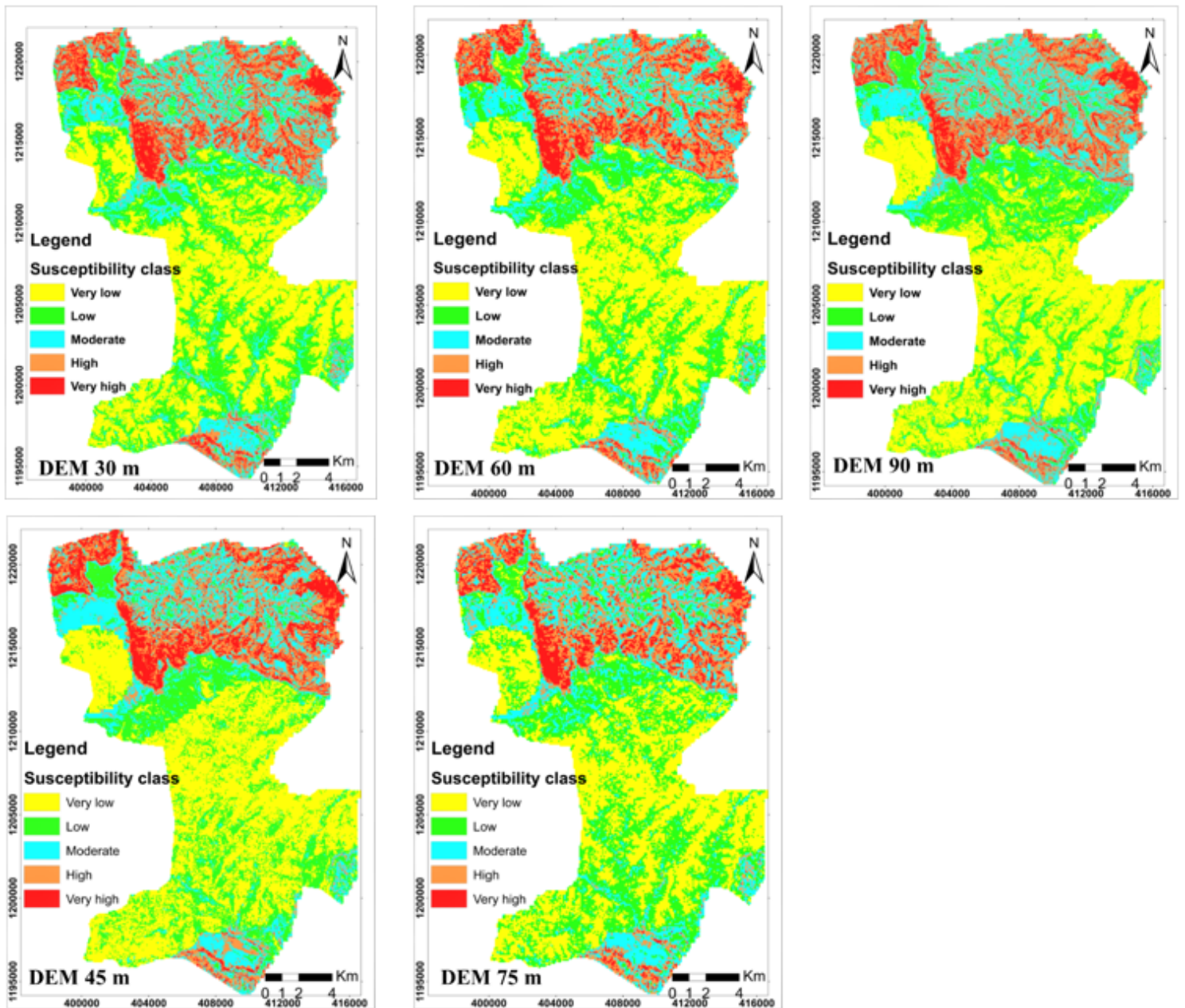
Figure 5

landslide susceptibility maps of five DEM resolution using the frequency ratio method
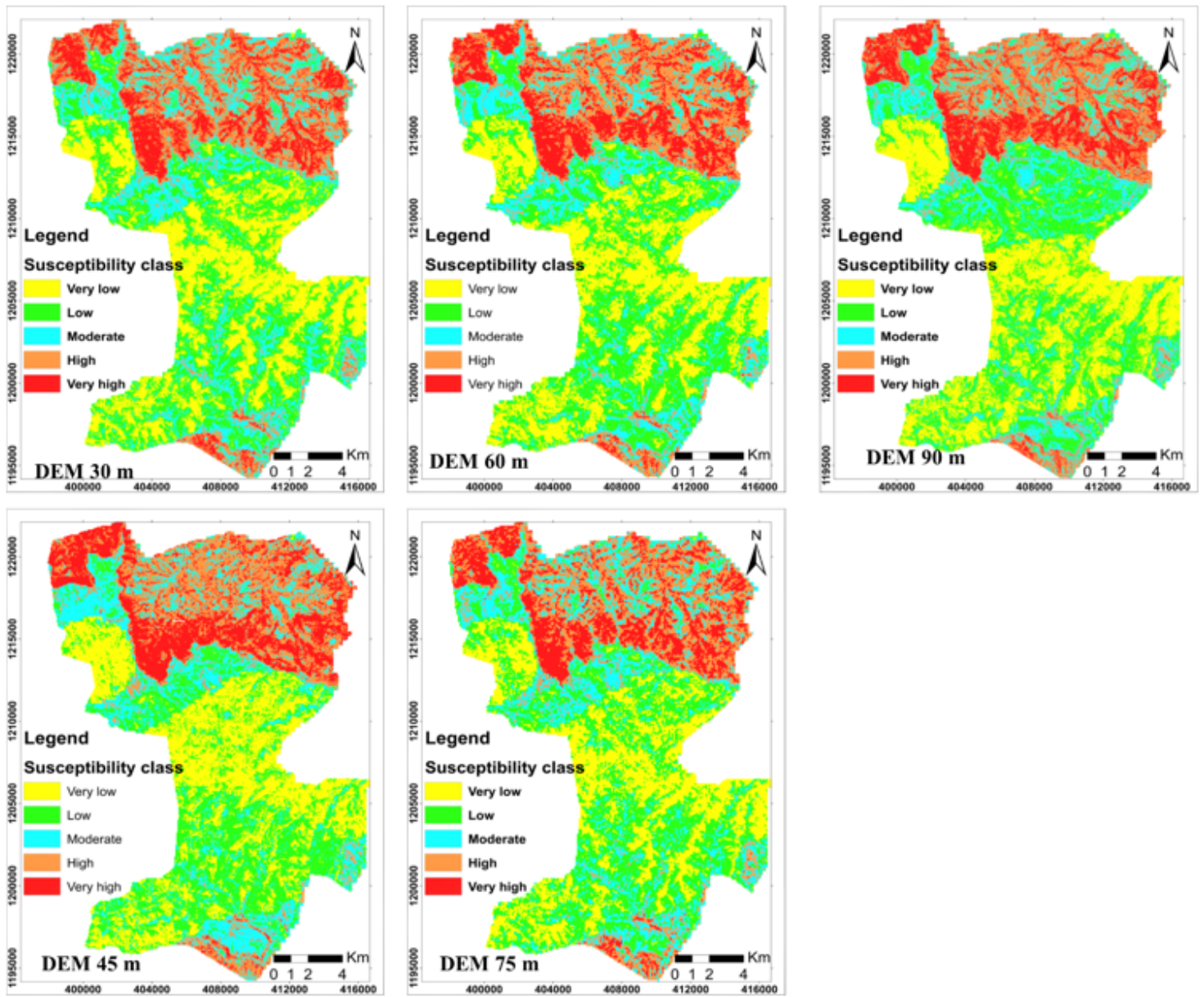
Figure 6

Landslide susceptibility maps of five DEM resolution using the certainty factor method
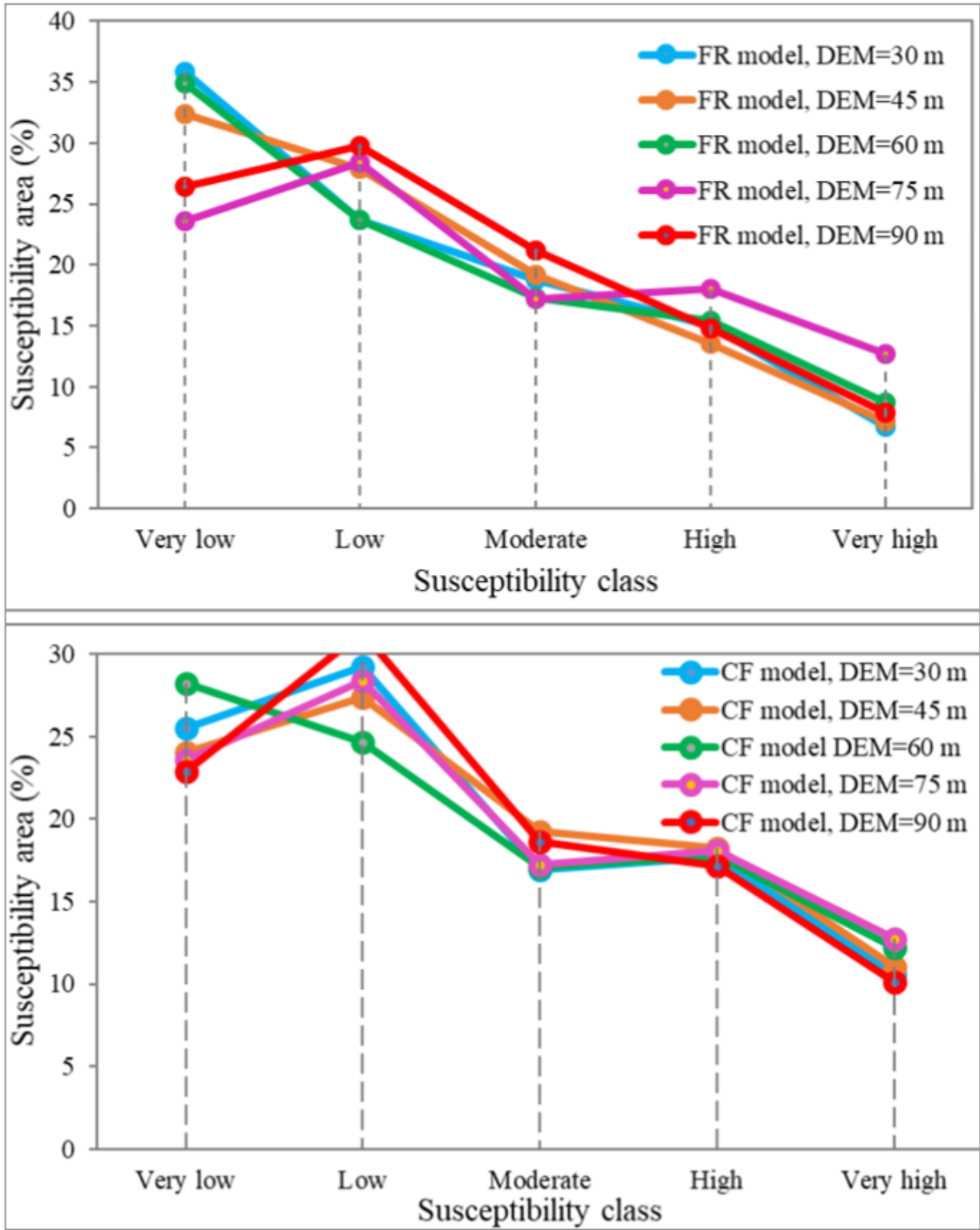
Figure 7

Landslide susceptibility area distribution of each five DEM resolutions for frequency ratio (FR) and certainty factor (CF) methods
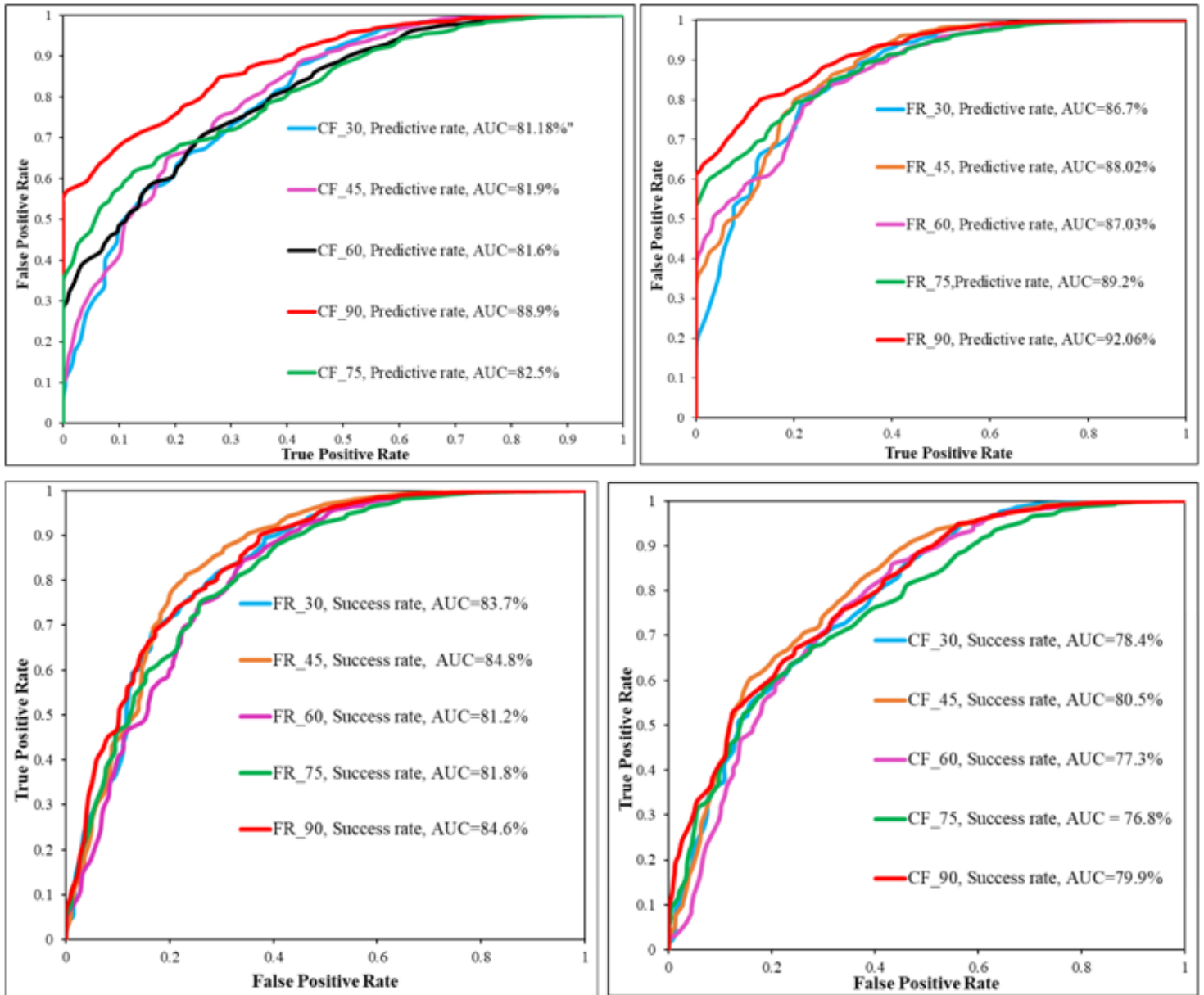
Figure 8

Receiver operating characteristics curve (ROC) of success and predictive rate curve for FR and CF methods
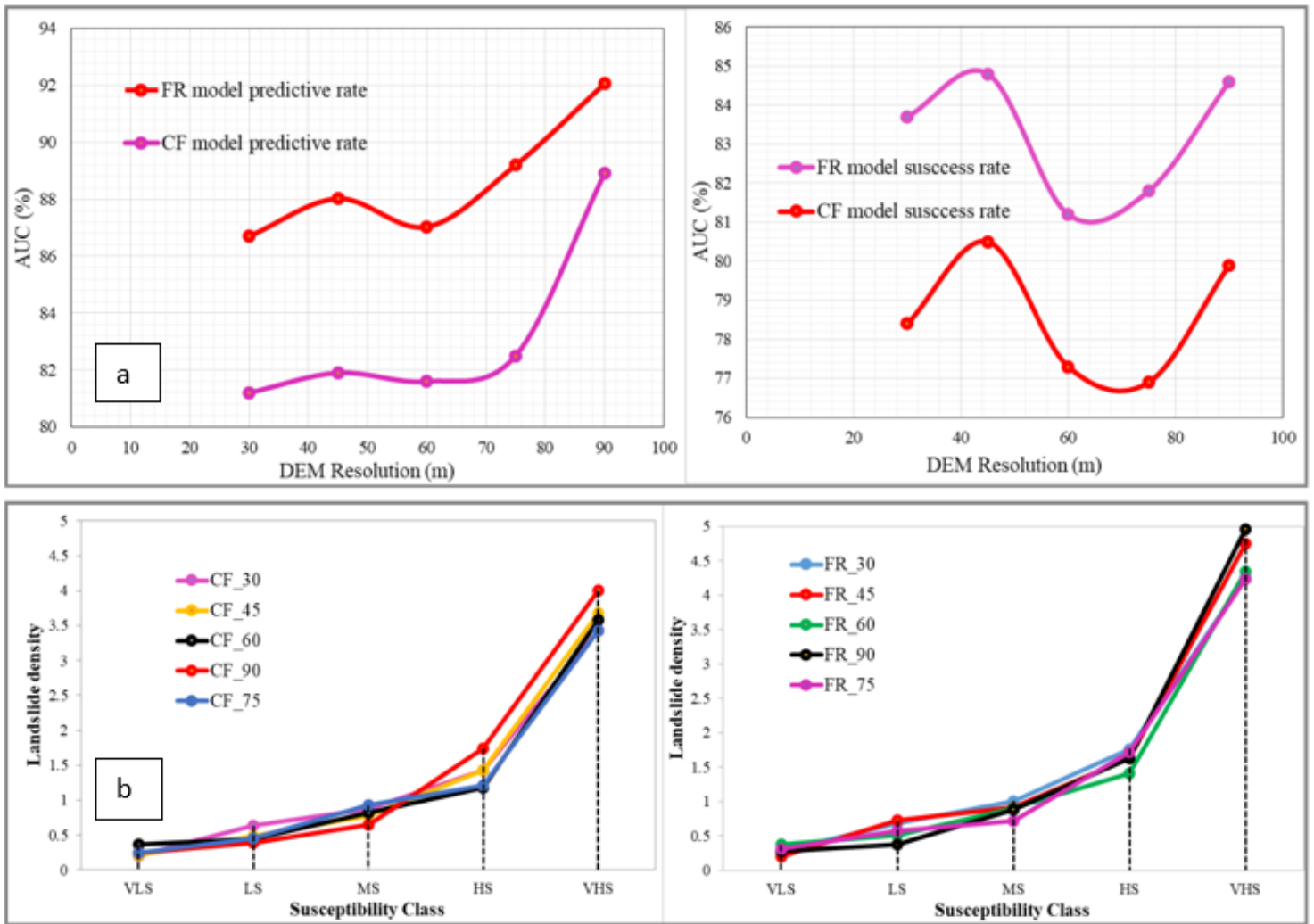
Figure 9

a) Area under the curve (AUC) and DEM resolutions and b) landslide density and susceptibility classes relationship